Int. J. Electrochem. Sci., 12 **(2017)** 11594 – 11601, doi: 10.20964/2017.12.81

International Journal of
ELECTROCHEMICAL
SCIENCE
www.electrochemsci.org

Low Temperature Synthesis of $SrCe_{0.9}Eu_{0.1}O_{3-\alpha}$ by Sol-Gel Method and $SrCe_{0.9}Eu_{0.1}O_{3-\alpha}$-NaCl-KCl Composite Electrolyte for Intermediate Temperature Fuel Cells

Ruijuan Shi, Junlong Liu, Hongtao Wang[*]*, Fufang Wu, Hui Miao, Yumin Cui*[**]

School of Chemical and Material Engineering, Fuyang Normal College; Anhui Provincial Key Laboratory for Degradation and Monitoring of Pollution of the Environment, Fuyang 236037, China
[*]E-mail: hongtaoking3@163.com, cymlh@126.com

Received: 22 August 2017 / *Accepted:* 13 October 2017 / *Published:* 12 November 2017

$SrCe_{0.9}Eu_{0.1}O_{3-\alpha}$ (SCEu-SG) electrolyte was prepared via the sol-gel method at a low heat-treating temperature of 1100 ^{o}C. The transport properties of SCEu-SG are studied using gas concentration cells. The results indicate that the protonic conduction of SCEu-SG is good in hydrogen-containing atmospheres. $SrCe_{0.9}Eu_{0.1}O_{3-\alpha}$-NaCl-KCl (SCEu-SG-NK) composite electrolyte was also fabricated and tested at between 500-700 °C. The conductivity of SCEu-SG-NK was observed to be 1.44×10^{-1} $S\cdot cm^{-1}$ in dry nitrogen at 700 °C. A maximum power density of 207 $mW\cdot cm^{-2}$ at 700 °C was achieved for the fuel cell based on the SCEu-SG-NK composite electrolyte which is much higher than that of single cerium strontium material, SCEu-SG (13.1 $mW\cdot cm^{-2}$).

Keywords: $SrCe_{0.9}Eu_{0.1}O_{3-\alpha}$(SCEu-SG); Composite electrolyte; Fuel cell; Ceramics; sol-gel preparation

1. INTRODUCTION

With the advantages of high efficiency, long-term stability, fuel flexibility, and low cost, solid oxide fuel cells (SOFCs) are recognized as the most perspective electrochemical conversion device with a solid oxide or ceramic electrolyte [1-2]. The perovskite-structured oxides such as $SrCeO_3$- and $BaCeO_3$-based materials have excellent protonic conduction at high temperatures [3-5]. The $SrCeO_3$-based perovskite ceramics exhibit higher protonic conduction than that of $BaCeO_3$-based perovskite ceramics in the high temperature range. Traditionally, the approach for the synthesis of $SrCeO_3$-based electrolyte is high-temperature solid state reaction which is a simple preparation method and encourages the production of a large amount of powder, but a high sintering temperature is required (≥

1500 ^{o}C) for the full densification of solid electrolyte. [6-9]. A recent study found that a novel solid state reaction method is used to synthesize nano-structured $Ce_{0.8}Er_{0.2-x}La_xO_{1.9}$ and the maximum conductivity of $Ce_{0.8}Er_{0.18}La_{0.02}O_{1.9}$ solid electrolyte which sintered at the optimum temperature of 1250°C reached 3.5×10^{-2} S·cm^{-1} at 800 ^{o}C [10]. In recent years, the sol-gel method has been widely used for the synthesis of $SrCeO_3$-based electrolyte [4,6,11]. The sol-gel process usually takes place under mild reaction conditions, the reactants can be uniformly mixed at the molecular level and pure, homogeneous and fine perovskite powders can be obtained easily at lower temperature.

Compared to high temperature fuel cells (HTFCs), intermediate temperature fuel cells (ITFCs) have generally been accepted in the commercialization of fuel cells (FCs), owing to their outstanding virtues such as excellent mechanical and thermal properties, high conductivity, long life and low cost [12-14]. Hence, novel composite electrolytes, such as ceria-carbonates or ceria-chlorides, which operate in an intermediate temperature range (400–700 °C) have been researched extensively [15-21]. In past years, $SrCeO_3$-based oxides focused on high temperatures between 600 and 1000 °C have received widespread attention [6-11]. However, to the best of our knowledge, there are very few reports on intermediate temperature (500–700 °C) electrical properties of doped $SrCeO_3$-inorganic salt composite electrolytes. $SrCe_{0.9}Yb_{0.1}O_{3-\alpha}$-NaCl-KCl composite electrolyte was found to display higher fuel cell performance than $SrCe_{0.9}Yb_{0.1}O_{3-\alpha}$-$Li_2CO_3$-$K_2CO_3$ and $SrCe_{0.9}Yb_{0.1}O_{3-\alpha}$-NaCl-$CaCl_2$ electrolytes in our previous study [22].

In this study, we synthesized $SrCe_{0.9}Eu_{0.1}O_{3-\alpha}$ (SCEu-SG) at a low temperature of 1100 ^{o}C via the sol-gel method. Then, $SrCe_{0.9}Eu_{0.1}O_{3-\alpha}$-NaCl-KCl (SCEu-SG-NK) composite electrolyte was developed. The structural and morphological properties of the electrolytes were investigated by a variety of characterization methods. The conduction behaviors of SCEu-SG-NK composite electrolyte in intermediate temperature (500–700 °C) were investigated and H_2/O_2 fuel cell was also tested.

2. EXPERIMENT

$SrCe_{0.9}Eu_{0.1}O_{3-\alpha}$ (SCEu-SG) electrolyte was prepared through the sol-gel method using citric acid as a sequestering agent. Firstly, Eu_2O_3 was dissolved by stirring in concentrated nitric acid and the stoichiometric $Sr(C_2H_3O_2)_2$ and $(NH_4)_2Ce(NO_3)_6$ were dispersed into deionized water. They were then added to the citric acid solution with the molar ratio of citric acid/total metal ions at 3. The solution pH was adjusted with NH_4OH solution to 8.0 and the obtained solution was then evaporated at 90 °C for 5 h to give a gel. The gel was dried at 120 °C for 12 h and heated for ashing treatment [4,6,11]. The resultant ash was calcined at 1100 °C for 5 h to obtain SCEu-SG electrolyte.

The molten salt of NaCl/KCl (50 mol% NaCl : 50 mol% KCl) was obtained and heated at 720 °C twice [23]. 80 wt% $SrCe_{0.9}Eu_{0.1}O_{3-\alpha}$-20 wt% (Na/K)Cl powder was then mixed and ground thoroughly. The resulting powder was uniaxially pressed into disks under pressure of 200 MPa and sintered at 750 °C for 1 h to obtain $SrCe_{0.9}Eu_{0.1}O_{3-\alpha}$-NaCl-KCl (SCEu-SG-NK) composite electrolyte. For a comparison, the SCEu-SG pellet was fabricated at 1500 °C for 5 h [22].

The microstructures of SCEu-SG and SCEu-SG-NK were observed by scanning electron microscope (SEM). The powder X–ray diffraction (XRD) pattern of samples was determined with a Panalytical X′ Pert Pro MPD diffractometer using Cu K_α radiation (λ=0.15418 nm).

To study the ionic conduction of the SCEu-SG under hydrogen-containing atmospheres, the observed electromotive forces (EMF_{obs}) of water vapor and hydrogen concentration cells using SCEu-SG as electrolyte and porous 20%Pd-80%Ag paste as anode and cathode were investigated in the temperature range of 500 to 700 °C and calculated as [24-25].

$$EMF_{obs} = \frac{RT}{2F} \{-t_{ion} \ln[p_{H_2(A)} / p_{H_2(B)}] + t_O \ln [p_{H_2O(A)} / p_{H_2O(B)}]\} \quad (1)$$

The conductivities of SCEu-SG and SCEu-SG-NK as a function of temperature in nitrogen atmospheres were tested on an electrochemical analyzer (CHI660E, made in China) in the temperature range of 500–700 °C. Silver wires with 20%Pd-80%Ag paste were applied as electrodes on both sides (with area of 0.5 cm^2) of the electrolytes. The effect of oxygen partial pressure (pO_2) on the conductivities was measured with a gas mixture of O_2, air, N_2 and H_2 in proper ratio using an oxygen sensor. The H_2/O_2 fuel cells of SCEu-SG and SCEu-SG-NK were also established.

3. RESULTS AND DISCUSSION

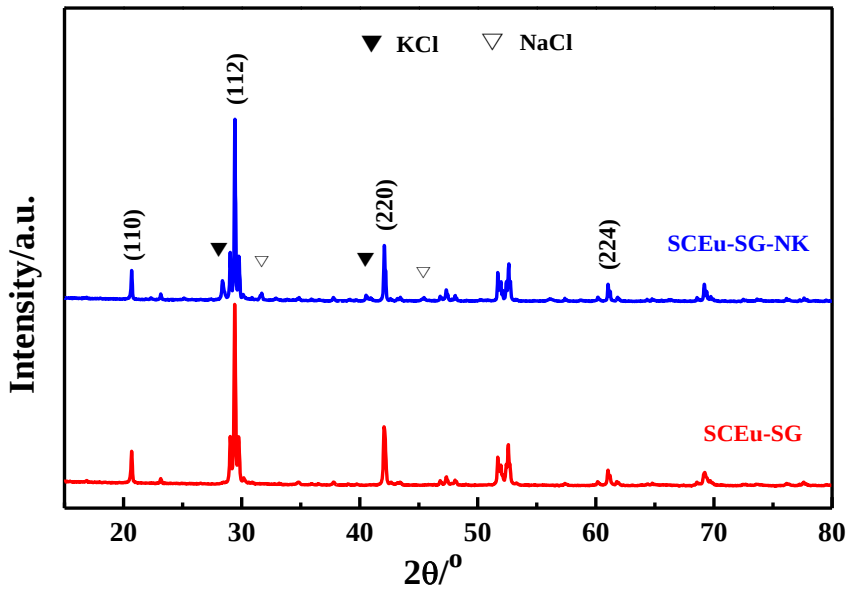

Figure 1. The XRD patterns of $SrCe_{0.9}Eu_{0.1}O_{3-\alpha}$ (SCEu-SG) and $SrCe_{0.9}Eu_{0.1}O_{3-\alpha}$-NaCl-KCl (SCEu-SG-NK).

The powder X–ray diffraction (XRD) patterns of SCEu-SG and SCEu-SG-NK are given in Fig. 1. All the peaks of the SCEu-SG are indexed to the cubic $SrCeO_3$ phase (JCPDS 01-082-2370). The diffraction peaks at 20.75 º, 29.48 º, 42.18 º and 61.13 º correspond to the (110), (112), (220) and (224) crystal planes of $SrCeO_3$, respectively. As is clearly shown in Fig. 1, SCEu-SG-NK composite electrolyte exhibited the same diffraction peaks and are agree well with the SCEu-SG phase. But the

peaks of NaCl (JCPDS 01-072-1668) and KCl (JCPDS 01-073-0380) were also detected. However, peaks for NaCl and KCl are very small. It may be due to during the crystallization process of the sintered composites from 750 °C down to room temperature, $SrCe_{1-x}Yb_xO_{3-\alpha}$ crystallized firstly come out of solution on the $SrCe_{1-x}Yb_xO_{3-\alpha}$ crystal nucleus, and then pure NaCl crystal, pure KCl crystal and amount of amorphous NaCl-KCl eutectic phase come out of solution due to the partly miscibility in NaCl-KCl solid-state binary. That is to say, the SCYbx-NK composite electrolytes is a mixture of more fine and dense $SrCe_{1-x}Yb_xO_{3-\alpha}$, a portion of crystalline NaCl and KCl, and some amorphous NaCl-KCl eutectic phase. It can be deduced that there was no reaction between SCEu-SG and the inorganic salts during heat treatment [15-20].

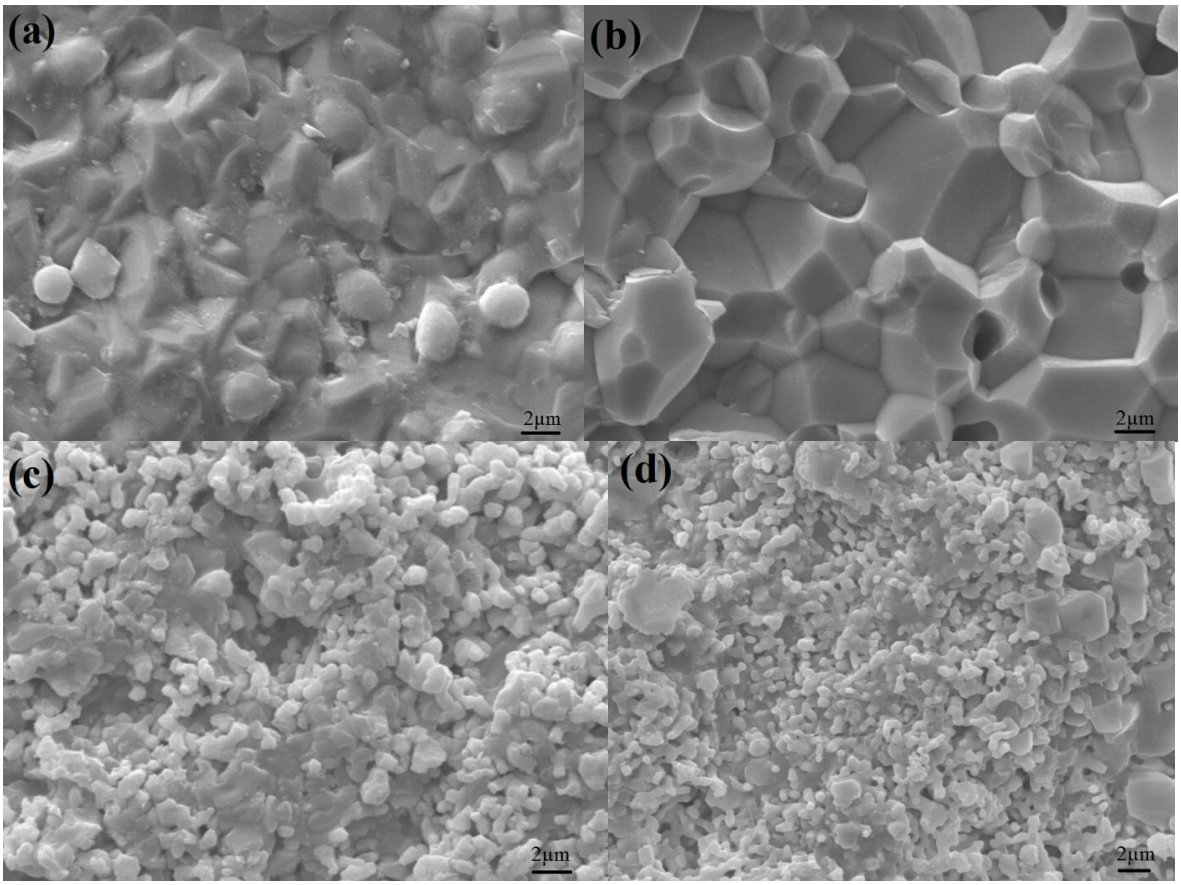

Figure 2. The surface and cross-sectional SEM images of SCEu-SG (a, b) and SCEu-SG-NK (c, d).

The surface and cross-sectional SEM images of SCEu-SG are displayed in Fig. 2(a,b). Fig. 2(a) demonstrates that the SCEu-SG is dense and free of cracks after being calcined at 1500 °C for 5 h. The cross-sectional image (Fig. 2(b)) shows that the morphology of SCEu-SG grains is uniform and dense, but there are some closed pores in the crystalline structures [6-10]. Fig. 2(c,d) illustrates the surface and cross-sectional morphologies of SCEu-SG-NK. Apparently, $SrCe_{0.9}Eu_{0.1}O_{3-\alpha}$ particles are linked to each other and their surface is uniformly covered by NaCl/KCl after sintering at 750 °C for 1 h [21]. Moreover, the $SrCe_{0.9}Eu_{0.1}O_{3-\alpha}$ particle size is smaller than in our previous report [22]. In summary, the wet chemical synthesis method (the sol-gel method) is quite favorable for the formation of uniform nanoparticles with relatively high surface area, but the density of particles, which is the key to the

performance of the SOCFs, was not high compared to the high-temperature solid state reaction method.

In the hydrogen-containing atmosphere, water vapor and hydrogen concentration cells were fabricated as follows.

H_2 (p_{H_2O} = 2.34×10^3 Pa), Pt| $SrCe_{0.9}Eu_{0.1}O_{3-\alpha}$| Pt, 30 % H_2 (p_{H_2O} = 2.34×10^3 Pa) (cell A)

H_2 (p_{H_2O} = 2.34×10^3 Pa), Pt| $SrCe_{0.9}Eu_{0.1}O_{3-\alpha}$| Pt, H_2 (p_{H_2O} = 1.23×10^4 Pa) (cell B)

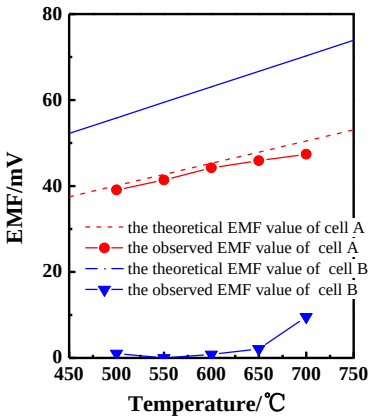

Figure 3. EMFs of hydrogen concentration cell (cell A) and EMFs of water vapor concentration cell (cell B) of $SrCe_{0.9}Eu_{0.1}O_{3-\alpha}$ (SCEu-SG) at 500-700 °C.

As can be seen from Fig. 3, transport numbers of total ions ($t_{ion} = t_H + t_O = EMF_{obs} / EMF_{cal}$) as high as approximately 0.94–0.98 were obtained by using hydrogen concentration cell (cell A) at 500–700 °C and are very close to the theoretical electromotive forces EMF_{cal} value ($EMF_{cal} = \frac{RT}{2F} \ln [p_{H_2(A)} / p_{H_2(B)}]$) of the hydrogen concentration cell. Similarly, the transport numbers of the oxide ions (t_O) is 0.00–0.14 at 500–700 °C were calculated in the water vapor concentration cell (cell B). These results demonstrate that the protonic conduction of SCEu-SG is good in a hydrogen-containing atmosphere, and there is a certain degree of oxide ionic conduction [26].

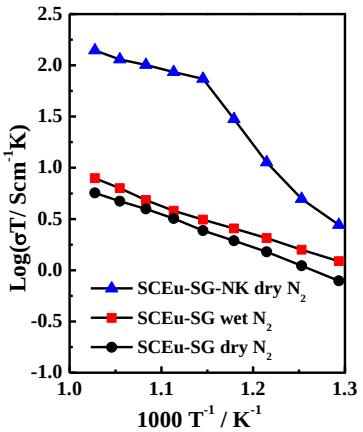

Figure 4. The plots of log (σT) ~ 1000 T^{-1} of $SrCe_{0.9}Eu_{0.1}O_{3-\alpha}$ (SCEu-SG) and $SrCe_{0.9}Eu_{0.1}O_{3-\alpha}$-NaCl-KCl (SCEu-SG-NK) from 500 to 700 °C in nitrogen atmospheres.

Fig. 4 presents the plots of log (σT) ~ 1000 T^{-1} of $SrCe_{0.9}Eu_{0.1}O_{3-\alpha}$ (SCEu-SG) and $SrCe_{0.9}Eu_{0.1}O_{3-\alpha}$-NaCl-KCl (SCEu-SG-NK) from 500 to 700 °C in nitrogen atmospheres. Apparently, the conductivity of SCEu-SG-NK is much higher than that of SCEu-SG in dry nitrogen and the highest conductivity is observed to be 1.44×10^{-1} $S\cdot cm^{-1}$ for SCEu-SG-NK at 700 °C. It was demonstrated that the introduction of NaCl/KCl molten mixture improved the effective concentration and conduction velocity of oxygen vacancy [16,18]. Besides, the conductivity plot of the composite electrolyte exhibits an elongated "Z"-type shape, which is consistent with the reported results [15,16].

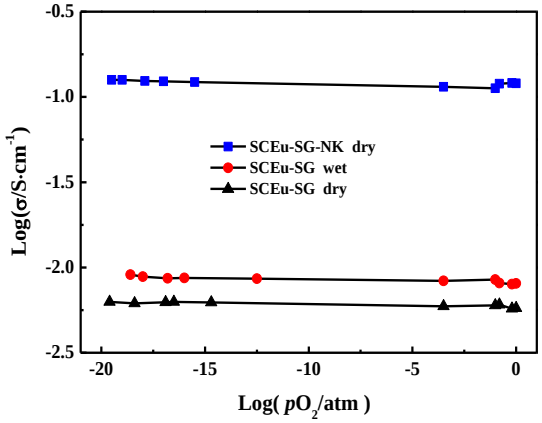

Figure 5. The conductivities of $SrCe_{0.9}Eu_{0.1}O_{3-\alpha}$ (SCEu-SG) and $SrCe_{0.9}Eu_{0.1}O_{3-\alpha}$-NaCl-KCl (SCEu-SG-NK) as a function of pO_2 at 700 °C.

To explore the ionic conduction of SCEu-SG and SCEu-SG-NK, the effect of oxygen partial pressure ($pO_2 = 10^{-20}$ ~ 1 atm) on the conductivities was also investigated. Fig. 5 shows the log σ ~ log (pO_2) plots of SCEu-SG and SCEu-SG-NK in dry and wet atmospheres at 700 °C. No, or only a slight change was observed in the conductivity with pO_2, which indicates that all the three electrolytes are pure ionic conductors. In the case of the SCEu-SG-NK composite electrolytes, the mobility of softened NaCl/KCl and $H^{\bullet}$, O^{2-} greatly enhances at the cell operation temperature of 700 °C which leads to a reduction of activation energy for ion transport through the interface of the $SrCe_{0.9}Eu_{0.1}O_{3-\alpha}$ and NaCl/KCl molten salts [27].

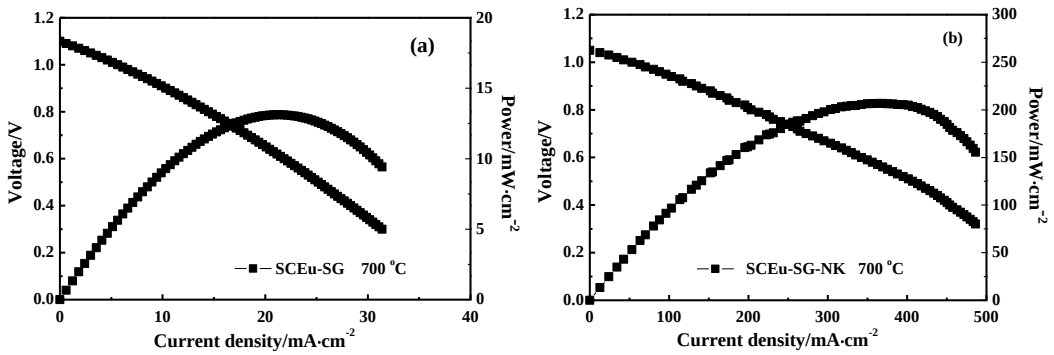

Figure 6. I-V and I-P curves for the H_2/O_2 fuel cells with SCEu-SG (a) and SCEu-SG-NK (b) electrolytes at 700 °C.

The cell performance was studied using hydrogen as fuel and oxygen as oxidant for SCEu-SG and SCEu-SG-NK at 700 °C, and is shown in Fig. 6.

As can be seen in Fig. 6(b), the open circuit voltage is approximately 1.06 V, which is very approximate to the theoretical value [22]. The results agree well with the SEM, that the NaCl/KCl eutectic melt is bound to the surface of SCEu-SG during the heat treatment, causing the dense texture. The fuel cell based on SCEu-SG-NK generated the maximum power output density of 207 $mW \cdot cm^{-2}$ at 700 °C which is remarkably higher than that of SCEu-SG (13.1 $mW \cdot cm^{-2}$ in Fig. 6(a)). Such performance can be attributed to the highly ionic conducting composite electrolyte, and makes the SCEu-SG-NK a suitable and promising electrolyte material for an intermediate temperature fuel cell.

4. CONCLUSIONS

In this work, novel $SrCe_{0.9}Eu_{0.1}O_{3-\alpha}$ was successfully prepared through the sol-gel method at a low temperature of 1100 ^{o}C for the first time. The surface and cross-sectional morphologies of SEM show $SrCe_{0.9}Eu_{0.1}O_{3-\alpha}$ is dense and free of cracks after being calcined at 1500 °C for 5 h. $SrCe_{0.9}Eu_{0.1}O_{3-\alpha}$ particles are linked to each other with NaCl/KCl covered uniformly after sintering at 750 °C for 1 h. The highest conductivity was observed to be 1.44×10^{-1} $S \cdot cm^{-1}$ for SCEu-SG-NK in dry nitrogen at 700 °C. The plots of log $\sigma \sim$ log (pO_2) indicate that SCEu-SG and SCEu-SG-NK are almost pure conductors of ion. The fuel cell based on the SCEu-SG-NK composite electrolyte displayed a good performance compared to the SCEu-SG, with a maximum power output density of 207 $mW \cdot cm^{-2}$ at 700 °C.

ACKNOWLEDGEMENTS
This work was supported by the National Natural Science Foundation of China (No. 51402052, 21402029, 21602029) and the Natural Science Foundation of Department of Education of Anhui Province (2015KJ008).

References

1. S. Su, S. Zhang, C. Yan, Z. Yang, F. Zheng and L. Zhang, *Int. J. Electrochem. Sci.*, 12 (2017) 230.
2. L. Fang, *Int. J. Electrochem. Sci*., 12 (2017) 218.
3. G. S. Reddy and R. Bauri, *J. Alloy Compd*., 688 (2016) 1039.
4. W. Xing, P.I. Dahl, L.V. Roaas, M.-L. Fontaine, Y. Larring, P.P. Henriksen and R. Bredesen, *J. Membrane Sci.*, 473 (2015) 327.
5. J. Xiao, L. Chen, H. Yuan, L. Ji, C. Xiong, J. Ma and X. Zhu, *Mater. Lett.*, 189 (2017) 192.
6. I.-M. Hung, Y.-J. Chiang, J. S.-C. Jang, J.-C. Lin, S.-W. Lee, J.-K. Chang and C.-S. His, *J. Eur. Ceram. Soc.*, 35 (2015) 163.
7. C. Liu, J.-J. Huang, Y.-P. Fu, C. Li, J.-Y. Wang and S. Lee, *Ceram. Int.*, 41 (2015) 2948.
8. Y. Okuyama, K. Isa, Y.S. Lee, T. Sakai and H. Matsumoto, *Solid State Ionics*, 275 (2015) 35.
9. K.S. Knight, R. Haynes, N. Bonanos and F. Azough, *Dalton Trans.*, 44 (2015) 10773.
10. Q. Hu, F. Yang, H. Fang and C. Zhao, *Int. J. Electrochem. Sci.*, 12 (2017) 7411.
11. W. Yuan, C. Xiao and L. Li, *J. Alloy Compd.*, 616 (2014) 142.

12. C. Zhang and K. Huang, *J. Power Sources*, 342 (2017) 419.
13. C. Li, R. Dai, R. Qi, X. Wu and J. Ma, *Int. J. Electrochem. Sci*., 12 (2017) 2485.
14. M.K. Rath and K.-T. Lee, *J. Alloy Compd.*, 657 (2016) 537.
15. A.I.B. Rondao, S.G. Patricio, F.M.L. Figueiredo and F.M.B. Marques, *Int. J. Hydrogen Energ.*, 39 (2014) 5460.
16. S. Shawuti and M.A. Gulgun, *J. Power Sources*, 267 (2014) 128.
17. N.C.T. Martins, S. Rajesh and F.M.B. Marques, *Mater. Res. Bull.*, 70 (2015) 449.
18. B. Zhu, S. Li and B.E. Mellander, *Electrochem. Commun.*, 10 (2008) 302.
19. Q.X. Fu, W. Zhang, R.R. Peng, D.K. Peng, G.Y. Meng and B. Zhu, *Mater. Lett.*, 53 (2002) 186.
20. Q.X. Fu, S.W. Zha, W. Zhang, D.K. Peng, G.Y. Meng and B. Zhu, *J. Power Sources*, 104 (2002) 73.
21. J.T. Kim, T.H. Lee, K.Y. Park, Y. Seo, K.B. Kim, S.J. Song, B. Park and J.Y. Park, *J. Power Sources*, 275 (2015) 563.
22. W. Zhang, M. Yuan, H. Wang and J. Liu, *J. Alloy Compd.*, 677 (2016) 38.
23. X. Liu, N. Fechler and M. Antonietti, *Chem. Soc. Rev.*, 42 (2013) 8237.
24. J. Guan, S.E. Dorris, U. Balachardran and M. Liu, *Solid State Ionics*, 100 (1997) 45.
25. X. Chen, C.S. Wang, E.A. Payzant, C.R. Xia and D. Chu, *J. Electrochem. Soc.*, 155 (2008) B1264.
26. H. Wang, H. Zhang, G. Xiao, F. Zhang, T. Yu, J. Xiao and G. Ma, *J Power Sources*, 196 (2011) 683.
27. C. Slim, L. Baklouti, M. Cassir and A. Ringuedé, *Electrochim. Acta*, 123 (2014) 127.